Preprints of the 21st IFAC World Congress (Virtual)
Berlin, Germany, July 12-17, 2020

Active Control of the Reliability of Wind Turbines

Niklas Requate * **Tobias Meyer** *

* *Fraunhofer Institute for Wind Energy Systems IWES, Am Luneort 100, 27572 Bremerhaven, Germany (e-mail: niklas.requate@iwes.fraunhofer.de)*

Abstract: Wind turbines operation is always a trade-off between reliability and functionality. A turbine's main functionality is power generation, but this induces loads on the structure. These ultimately lead to damage and thus reduce reliability. A suitable trade-off for safe and prolonged operation needs to be found during the design process. During operation, however, the selected trade-off will not be ideal for each individual turbine because of site specific influences. Multiple trade-offs can be obtained with different turbine controller configurations. These allow for an adaptation to the individual reliability and functionality of a specific wind turbine. A closed loop supervisory reliability control for wind turbines is implemented and tested. It is based on a feedback of the current turbine condition and continuously selects the optimal controller from a predefined set of controller configurations. Simulations are conducted to evaluate the effect of reliability control on wind turbine reliability and power production over several years of operating time. Results show that a desired reliability of a wind turbine can be actively controlled even on a slow time scale and with a small number of feasible turbine controller configurations. Reference tracking is sufficiently good despite uncertain wind conditions.

Keywords: reliability control, self adapting systems, wind turbine control, supervisory control

1. INTRODUCTION

Wind turbines are operated with a single main objective: Maximization of monetary profit. During operation, the major cost driver, which diminishes monetary profit, is maintenance due to low reliability. The major contributor is power generation. Generally, reliability as well as functionality is assured during design of a wind turbine. Functional requirements are tested either model-based or using prototypes. Meeting reliability requirements is more challenging, as all test methods rely on changed operating conditions and need to excite the relevant failure modes. Ultimately, reliability requirements can only be validated once the product is put into use. With well-known nominal reliability and low safety margins, usage and functionality of a wind turbine have a major influence on actual reliability. This results in large variance in actual time to failure.

Wind turbines pose the additional challenge that reliability requirements can only be fulfilled by including active load reduction techniques in turbine control. For single turbines, Njiri and Söffker (2016) is a good overview of existing solutions. In principle, these low-level controllers can be adapted in order to fulfill nominal reliability requirements of an individual turbine. This adjusts the trade-off between functionality and reliability during operation. However, the gap from high-level profit maximization to low-level turbine control is too large to be covered directly. Instead, we propose to use reliability control to adapt turbine behavior, see Meyer (2016). It allows for a more abstract selection of the trade-off between reliability and functionality and thus makes separate high-level profit maximization schemes possible.

Each wind turbine has an individual fatigue life budget due to manufacturing tolerances. Additionally, the site specific wind conditions impose different loads on each wind turbine. This holds true especially in wind farms, where the tight spacing of wind turbines leads to greatly differing wind conditions. Galinos et al. (2016) clearly shows that each turbine experiences individual loads despite being subjected to common wind farm inflow conditions. Bossanyi (2018) presents an approach to consider fatigue loads as well as energy production as setpoints for the wind farm controller. In Beganovic et al. (2018), an adapted control strategy to reduce structural loads by means of online fatigue damage evaluation is proposed for a single wind turbine. This information is used to select different controller configurations of the wind turbine real-time controller. However, the approach is not tested for a long period of time with varying wind conditions and the strategy to select the setpoint choice of the controller configuration is not elaborated. In Meyer et al. (2017), the application of reliability control to wind turbines and wind farms is proposed. In this paper, the implementation and validation of this approach for a generic 7.5 MW wind turbine is presented. Section 2 gives an overview on the structure of the reliability controller for wind turbines. The selection of low-level controller configurations is described in Section 3. The implementation of the model-predictive reliability controller is presented in Section 5. For design and verification of the proposed approach, simulations over several years of operating time are needed. Results of such simulations with a reliability controlled wind turbine are presented in Section 5. Conclusions are drawn in Section 6.

2. STRUCTURE OF RELIABILITY CONTROL

Wind turbines are equipped with controllers for power, pitch and yaw and a multitude of other controllers that work in real-time and directly interact with the structure. Reliability control builds on these by adding an outer supervisory control loop as shown in Fig. 1. The outer loop requires extensive knowledge about the current system condition, which is provided by a comprehensive condition monitoring system for all relevant components. The outer loop interacts with the real-time controllers only by initiating a change of controller configuration. By implementing a two-stage control setup, the actual turbine controllers are separated from the reliability control loop. The turbine controllers run on their individual, very fast time scale, whereas the reliability controller works on a much slower time scale to cope with the slow degradation processes. The separation of the two stages brings some main advantages. It allows for using contemporary control design individually on both levels (wind turbine controller and reliability control). Additionally, a validation and certification of each selected wind turbine controller configuration becomes possible. The two different stages can also be found again in the development process of the reliability controller. At first, suitable control configurations need to be selected. In a second step, the reliability controller itself is designed and implemented.

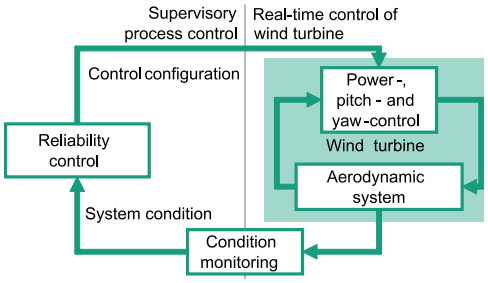

Fig. 1. Outline of reliability control loop for wind turbines

3. SELECTION OF REAL-TIME CONTROLLER CONFIGURATIONS

The reliability controller uses the feedback of the system condition of the wind turbine as controllable quantity. However, the system condition of a wind turbine is not a single quantity but consists of various failure modes for various components. Ideally, the reliability controller can control all failure modes of the wind turbine at the same time while keeping the energy production of the turbine as high as possible. Therefore, a set of controller configurations needs to be found where each configuration represents an optimal trade-off between the failure modes and energy. A multiobjective optimization problem can be formulated where n performance parameters of the real-time controllers are selected as optimization variables $x \in P \subset \mathbb{R}^n$. The objective functions $f : P \to \mathbb{R}^m$ represent the influence of controller configurations on $m-1$ failure modes and energy production throughout the entire lifetime of a wind turbine. The Pareto-optimal solution is then found by solving

$$\begin{aligned} \min_{x \in \mathbb{R}^{n_x}} \quad & f(x) = (f_1(x), f_2(x), \ldots, f_m(x)) \\ \text{subject to} \quad & h(x) = 0 \\ & g(x) \leq 0. \end{aligned} \tag{1}$$

The functions $h\colon P \to \mathbb{R}^{n_h}$ and $g\colon P \to \mathbb{R}^{n_g}$ are used optionally to express equality and inequality constraints to the optimization variables.

Whereas the quantification of produced energy of a wind turbine is fairly straightforward, the formulation of a quantifying measure for the reliability with regard to a specific failure mode is highly component specific and often requires complex models and simulations. During the design process of wind turbines, aero-elastic simulations of a wind turbine model including the real-time controllers are performed. Standard guidelines like IEC (2019) define dynamic load cases (DLCs) which specify sets of simulations for different operating and wind conditions. Those simulations are evaluated to estimate fatigue and ultimate loads in order to design components for the lifetime of 20 or 25 years. Ultimately, a complete set of DLCs would need to be performed for each candidate set of optimization variables. However, the high computational cost of these simulation stands in contradiction to the need for an efficient evaluation of objective functions for the multiobjective optimization problem. In addition, the complexity of reliability control increases with each failure mode that is considered. On the one hand, each additional failure mode adds another trade-off to balance for the reliability controller. On the other hand, it means that another objective function is added to the multiobjective optimization problem which also increases the complexity of solving it. Altogether, controller parameters, performed simulations and number of failure modes need to be selected such that a balance between computational effort and accuracy of results is maintained. Within this paper, we focus on showing the feasibility of reliability control for wind turbines. Therefore, we only consider one failure mode as objective besides energy production and also limit the number of controller parameters to two. The specific choices are described in the following subsections.

3.1 Choice of objectives

In order to show the functionality and advantages of reliability control for wind turbines, we use the fatigue loads of rotor blades, which are major, complex components of a turbine. Failures in rotor blades can range from minor cracks, which degrade aerodynamic performance, to structurally critical cracks in the main beam. Detailed degradation models are able to cover most of these by combining a finite-element model of the blade with an individual computation of fatigue loads for each element (see Shokrieh and Rafiee (2019)). However, the complexity of these models and their computational demands make them unsuitable for multiobjective optimization. A simpler approach summarizes the blade in a single value by means of the damage equivalent loads (DEL) of the blade root bending moment (see Sutherland (1999)). DEL calculation analyses fatigue loads by using Miner's rule, which assumes linear accumulation of individual hysteresis cycles. Even though applying this method to composite materials, such as rotor blades, is a strong simplification, a multitude of control designs that are based on blade

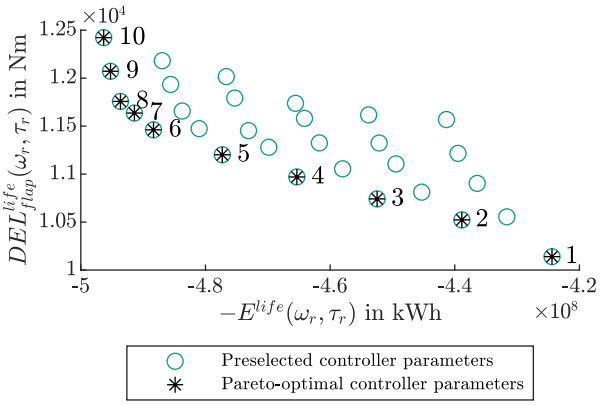

Fig. 2. Objective values of preselected configurations

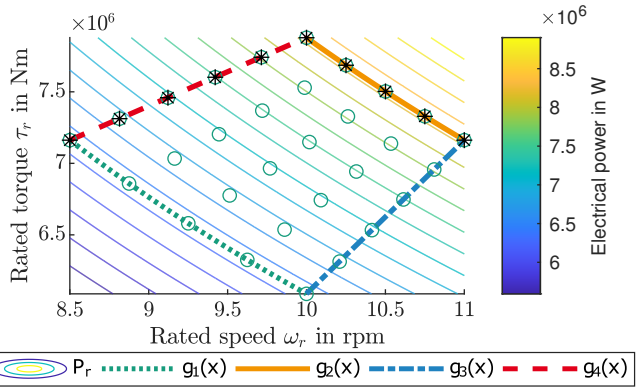

Fig. 3. Preselected combinations of rated generator torque and rated generator speed within the constraints

root bending moment fatigue loads can be found. As their number is so large, we wish not to source or highlight individual papers. For demonstration, we select the flapwise bending moment of a single rotor blade, since all three blades show the same behavior except for simulation irregularities. Flapwise bending moments are highly dependent on wind turbulences. By showing that it is still possible to control this quantity, a transfer to other failure modes is facilitated.

Summing up, two objective functions $f_1(x) = -E^{life}(x)$ and $f_2(x) = DEL^{life}_{flap}(x)$ are used for the optimization problem, where $E^{life}(x)$ denotes the predicted energy yield and $DEL^{life}_{flap}(x)$ the damage equivalent load, both for the design lifetime of the turbine. Required models and simulations are described in the following section followed by a discussion of the controller parameters x.

3.2 Wind turbine model and simulations performed in objective function

According to IEC (2019), the fatigue loads during normal operation are estimated by DLC 1.2. Wind conditions are defined by IEC (2019) for several different categories. They are characterized by their wind speed distribution and turbulence characteristics. To cover the whole range of wind speeds and turbulence intensities, separate simulations are required for each combination of these. Additionally, the influence of specific random turbulence realizations is limited by running several simulations with different random seeds, but nominal wind characteristics. In the realization of the objective function, we perform simulations using turbulent wind fields with a duration of 10 minutes each with 6 different seeds per mean wind speed. The mean wind speeds range from 4 m/s to 26 m/s in steps of 2 m/s. Turbulence is chosen according to IEC-class C. In total, 72 simulations are performed. Comparability between different controller parameter values is assured by using the same wind fields across all objective function evaluations. In this paper, we use the generic direct-drive IWT 7.5 MW onshore wind turbine (see Popko et al. (2018)). Aero-elastic simulations are performed with MoWiT (see Leimeister and Thomas (2017)). The rated power $P_{nom} = 7.5162$ MW is obtained at a rated rotational rotor speed of $\omega_{nom} = 10$ rpm and a rated generator torque of $\tau_{nom} = 71620$ MNm. These simulations are aggregated to a lifetime DEL by extrapolating and weighting each simulation result with the wind speed distribution. In order to comply with our evaluation site, IEC-class III wind conditions are employed. The Wöhler-coefficient for the linear damage accumulation of the blade root bending moments is set to 10 as is common for fibreglass materials (see Sutherland (1999)). The energy yield is also extrapolated to the design lifetime of 20 years with the probability distribution of mean wind speeds.

3.3 Choice of controller parameters

The real-time controller for the power production mode of a wind turbine is commonly designed to maximize power in the partial load region, i.e. below rated wind speed, and to maintain the rated power in the full load region above the rated wind speed (see Njiri and Söffker (2016), p.379). Above rated wind speed, a gain scheduled PI-controller is used to control the rotational speed by adapting the pitch angle of the blades. In addition, a constant generator torque is kept. In order to show a generally applicable approach to many wind turbine controllers, we use a controller without any additional features and select controller parameters which are needed in any wind turbine controller. Thus, optimization variables are the controller setpoints for the rated generator speed ω_r and the rated generator torque τ_r. This results in $x = (\omega_r, \tau_r)$. The product of the rated speed and rated torque yields the rated power $P_r = \omega_r \cdot \tau_r$ of the turbine neglecting any occurring losses. For the optimization problem, we specify that all three values ω_r, τ_r and P_r can be reduced by 15 % or increased by 10 % from the nominal values defined above. This leads to constraints on the optimization variables

$$0.85 \cdot \omega_{nom} \leq \quad \omega_r \leq 1.1 \cdot \omega_{nom} \tag{2}$$

$$0.85 \cdot \tau_{nom} \leq \quad \tau_r \leq 1.1 \cdot \tau_{nom} \tag{3}$$

$$0.85 \cdot \tau_{nom}\omega_{nom} \leq \tau_r\omega_r \leq 1.1 \cdot \tau_{nom}\omega_{nom}. \tag{4}$$

An increase or decrease of power is well possible with most current wind turbines. Power reduction is a basic requirement to allow for power curtailment by the grid operator. Some modern wind turbines also support short-term uprating of the wind turbine to gain more energy if environmental and machine conditions allow. From discussions with manufacturers, we assume that increasing the rated power by 10 % is possible. The lower limit of 15% will reduce loads sufficiently without having too much loss in energy. Both values can be adapted for each specific turbine and demand. In addition to the constraints

described above, combinations of extremely high torque with low rotational speeds and vice versa are avoided by introducing two additional linear inequality constraints which are shown in Fig. 3. The constraints on the rated power from (4) are defined by $g_1(x)$ and $g_2(x)$. $g_3(x)$ and $g_4(x)$ define linear functions through the maximum and minimum values for combinations of ω_r and τ_r. On each contour line, the same rated electrical power of the turbine is attained. All combinations within the border of these four lines are feasible. Having defined objective functions, objective variables as well as constraints, the optimization problem (1) is completely defined.

3.4 Solving the optimization problem

To solve an optimization problem, numerical multiobjective optimization algorithms can be employed. These aim to reduce the value of all objective functions until Pareto-optimality is reached, i.e. one objective function value can only be decreased at the cost of an increase in another objective function value. However, with a complex optimization problem, the computational effort due to many objective function evaluations is very high. To limit this effort, we forego the use of optimization algorithms and manually select a set of of 36 feasible configurations instead. Pareto-optimal configurations are found by performing a non-dominance test. This approach still yields results that are consistent with the requirements for reliability control. Whereas commonly a discrete set of controller configurations needs to be found and examined in more detail after the optimization algorithm was used, this process is done partially in advance in this case. Rated generator speed ω_r and rated generator torque τ_r are preselected by distributing them uniformly within the predefined constraints. In order to do so, 6 different setpoints for the rated electrical power are selected as

$$\begin{aligned} P_r &= (0.85, 0.9, 0.95, 1, 1.05, 1.1) \cdot P_{nom} \\ &= (6.375, 6.75, 7.125, 7.5, 7.875, 8.25)\, MW. \end{aligned}$$

For each value of P_r, 5 combinations of τ_r and ω_r are selected as shown in Fig. 3. Each green circle defines a combination of preselected rated generator speed and rated generator torque which is used by the wind turbine real-time controller. Simulations are performed with these configurations as described in Section 3.2 and the outcome is evaluated to obtain the objective function values $f_1(x) = -E^{life}(\omega_r, \tau_r)$ and $f_2(x) = DEL^{life}_{flap}(\omega_r, \tau_r)$. Fig. 2 shows the results of such evaluations in the objective space. The non-dominated solutions are indicated as black stars in the objective space in Fig. 2 as well as in the parameter space in Fig. 3. All Pareto-optimal controller configurations are located on the defined constraints $g_2(x)$ for maximum rated power and $g_4(x)$. Logically, the energy yield rises with a higher rated electrical power of the turbine. Among configurations with an equal value of rated power, controller configurations with a reduced rotational speed and a higher torque are preferred because the DEL of the flapwise bending moment is affected stronger by changes in the rotor speed than in the torque. Contrary to this, the actual energy yield is slightly higher for the same rated power when rated rotor speed is increased and rated torque is decreased. This effect is caused by more kinetic energy stored in the rotor, which is converted into more electrical energy when the wind speed drops. This effect causes that all configurations with $P_r = 8.25\ MW$, which is the maximum admissible power, are Pareto-optimal. However, a slight increase in energy is accompanied by a clearly larger increase in loads. Despite that, a slight increase of energy yield directly increases the profit of a turbine operator and using such a configuration can still be reasonable for certain situations. Therefore, these ten controller configurations can be used by a reliability controller. Structure and design of the reliability controller including applied methods to use the obtained results are described in the following section.

4. IMPLEMENTATION OF THE RELIABILITY CONTROLLER

The main goal of a reliability controller is to control the degradation of the turbine at the current time to match the desired degradation over time. Degradation is expressed as health index (HI), which is 100 % for a new turbine and 0 % at failure occurrence. It is defined as

$$HI = 1 - \frac{\text{Spent fatigue life budget}}{\text{Total fatigue life budget}}. \tag{5}$$

The trajectory of the health index over time is a major design variable of the reliability controller. It allows to adjust a turbine to its site, its load history and to seasonal changes. To adapt turbine operation to the desired health index HI_{des}, the most suitable controller configuration needs to be selected from the current health index HI_{cur} and the predicted environmental conditions. For this, we employ model predictive control (MPC). The main advantage of MPC for the problem at hand is its ability to take predictions about environmental conditions into account. This allows it to e.g. safeguard a turbine from a storm. The reliability controller time scale is entirely separate from the real-time wind turbine controller. It can act on an hourly or even just a daily basis. For the selection of controller configurations, a new parameter α is introduced. It is mapped to a position on the Pareto front. This way, it allows to change the most suitable compromise just by changing the value of α. Therefore, α is used as manipulative variable for the reliability controller.

4.1 Parameterization of the Pareto-Front

In the general case, an m-dimensional Pareto-front is possible. All feasible solutions are then in $\mathbb{R}^m$. The Pareto-front is the lower limit of all feasible solutions. As such it has dimension $\mathbb{R}^{m-1}$. Additionally, it is bounded in each direction. For the two-dimensional case presented in this paper, the Pareto-front is one-dimensional and bounded by the individual minima for each objective function. To construct a measure along the Pareto-front, the approach described in Krüger et al. (2013) is employed. It is based on a simplex that connects the bounds of the Pareto front which is assumed to be a continuous function at first. The α-value is the position along the simplex; the Pareto-point is selected perpendicular to the position along the simplex. The orthogonal projection of an α-value to the Pareto-front is called s-transformation and the inverse transformation s^{-1} maps a Pareto-point to an α-value. The α-values are selected so that $\alpha = -1$ yields

lowest DEL but also lowest energy, whereas $\alpha = 1$ yields maximum energy at the cost of maximum DEL.

For the implementation of a reliability controller, each of the selected N_P controller configurations can be uniquely defined by an index $k = 1, \ldots, N_P$ implying the selection controller parameters x_k of the real-time controller an a corresponding set of Pareto-points

$$(f_{1,k}, f_{2,k}) = (f_1(x_k), f_2(x_k)) \quad \forall k = 1, \ldots, N_p. \tag{6}$$

These are mapped to an α value between -1 and 1 by

$$\alpha_k = s^{-1}(f_{1,k}, f_{2,k}) \quad \forall k = 1, \ldots, N_p. \tag{7}$$

In Section 3.4 $N_p = 10$ controller configurations were selected. For the Pareto-point yielding lowest DEL

$$s^{-1}((f_{1,1}, f_{2,1})) = \alpha_1 = -1$$

is used and for maximum energy

$$s^{-1}((f_{1,10}, f_{2,10})) = \alpha_{10} = 1$$

All Pareto-points in between are sorted in ascending order of α (see Fig. 2). Before the use of the α-parametrization within the MPC-reliability controller is described in Section 4.3, the validation model of the wind turbine is defined in the following section.

4.2 Validation model

To evaluate feasibility of reliability control, evaluations over several years are required. Experimental validation of such a time span is impossible. Instead, a model-based approach is necessary. Additionally, a model that allows for simulation of long durations is also required for the prediction within the reliability control setup. For each time step, the damage increment is read from a lookup table which maps mean wind speed $v(t)$ and turbulence intensity $TI(t)$ to a damage increment at a time step Δt_{sim}. Multidimensional interpolation, additional mapping functions and corrections are used to determine the damage increment for an arbitrary wind condition from limited lookup table data. It is generated from more detailed simulations which were conducted with aero-elastic simulations and damage evaluations similar to those described in Section 3.2. In this case Miner's rule is applied to calculate the damage increment for a 10 minute time interval. The DEL-value of the nominal controller configuration (see Section 3.2) was used as ultimate load so that a damage value of 1 would be attained with the design lifetime of 20 years if the wind conditions were equal to the design wind conditions. In addition to damage increments, energy increments are computed as well. These are not directly required for reliability control, but allow for more in-depth performance evaluations. This approach builds the function $F : (v, TI, \alpha) \to \mathbb{R}$ which models the damage rate of the flapwise bending moment $\dot{D}(t)$. By integrating this value, the sustained damage, which is used as a measure for the spent fatigue life budget, is obtained. Relating it to the total fatigue life budget D_{nom} yields the current HI. The discrete value $\alpha_k(t)$, depending on the selected controller configuration at time t, is used in F:

$$\begin{aligned} \dot{D}(t) &= F(v(t), TI(t), \alpha_k(t)),\ k = 1, \ldots, N_p \\ HI_{cur}(t) &= 1 - \frac{D(t)}{D_{nom}}. \end{aligned} \tag{8}$$

The assumption for the damage accumulation described above determines a total fatigue life budget of $D_{nom} = 1$. The model (8) can be used for controller performance evaluation, but also for the prediction in MPC.

4.3 Model predictive reliability controller

The α-value that was described in Section 4.1 is used as manipulative variable of the reliability controller in order to control the HI of the failure mode, i.e. the flapwise bending moment in this case. The model predictive controller predicts the future behaviour from the current time t_c for a specified prediction horizon $T = p \cdot t_s$, where t_s is the time step of the controller and p is the number of prediction steps. By solving an optimal control problem, the optimal trajectory of the manipulative value

$$\alpha_{C,i} = \alpha_C(t_c + i \cdot t_s) \quad \forall i = 1, \ldots, p \tag{9}$$

is calculated for the prediction horizon and the first value $\alpha_{C,1}$ is used as controller output. The trajectory is obtained by minimizing the cost function

$$J = w_{HI} J_{HI} + w_\alpha J_\alpha, \tag{10}$$

where J_{HI} penalizes the error of the health index prediction and J_α high fluctuations of α_C. The parameters w_{HI} and w_α are used to weight the influence of the individual cost functions. J_{HI} is a metric for the deviation of predicted health index from desired health index:

$$J_{HI} = \sum_{i=1}^{p} \left(HI_{des}(t_c + i \cdot t_s) - HI_{pred}(t_c + i \cdot t_s)\right)^2 \tag{11}$$

The prediction HI_{pred} 1depends on the manipulating variable $\alpha_C(t)$ as well as on the predicted wind conditions denoted as $v_{pred}(t)$ and $TI_{pred}(t)$. The wind prediction is available with a time step t_w which can be different than the controller time step.

As mentioned before, a similar model as the validation model can be used. The HI needs to be a continuous function of α_C in this case, whereas separate models for each configuration k were used before. In order to do so, a linear fit of the damage value for each wind speed and turbulence with respect to the discrete alpha values from the N_p selected controller configurations is used. Linear interpolation is applied, as in the validation model, for wind speed and turbulence. The predicted HI is then obtained by

$$\begin{aligned} \dot{D}_{pred}(t) &= F_{pred}(v_{pred}(t), TI_{pred}(t), \alpha_C(t)) \\ HI_{pred}(t) &= 1 - \frac{D_{pred}(t)}{D_{nom}}. \end{aligned} \tag{12}$$

To reduce frequent changes of the controller configurations, the difference in successive values of α_C is also minimized by

$$J_\alpha = (\alpha_{cur} - \alpha_{C,1})^2 + \sum_{i=1}^{p-1} (\alpha_{C,i} - \alpha_{C,i+1})^2. \tag{13}$$

α_{cur} is the controller parameter that was used for the current time step t_c. The optimal system input for the prediction horizon is obtained by

$$(\alpha_{C,1}, \ldots, \alpha_{C,p}) = \underset{(\alpha_{C,1}, \ldots, \alpha_{C,p})}{\arg\min} \ J \tag{14}$$

with box constraints $-1 \leq \alpha_{C,i} \leq 1 \, \forall i = 1, \ldots, p$. The controller configuration k_{use} which is transferred to the wind turbine or the validation model respectively is found by selection of the closest value of $\alpha_1, \ldots \alpha_{N_p}$ to $\alpha_{C,1}$.

Fig. 4 shows the setup of the control loop including the MPC-reliability controller (MPC) and the wind turbine model (WT). Simulations with different design parameters of the controller and desired HI trajectories are performed using the validation model. Setup and parameters performed simulations are described in the following section.

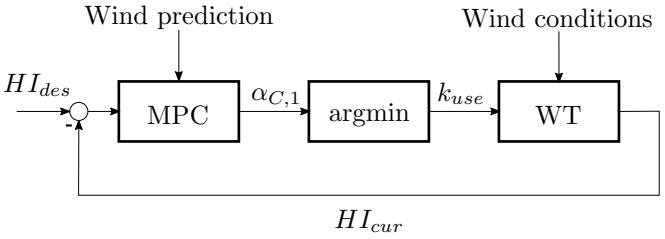

Fig. 4. Implemented reliability control loop

5. RESULTS

Application and testing of reliability control for wind turbines presents unique challenges. The validation model described in 4.2 allows to simulate several years of operation within a reasonable time. Regarding the reliability controller itself, the incoming wind speed and turbulence intensity act as disturbances and have a high impact on the controlled variable, i.e. the health index. In addition, the reliability control loop is not able to influence the degradation rate, and thus the health index, at all times. This is due to a fixed number of available configurations of the underlying real-time wind turbine controllers, which only affect the degradation rate at wind speeds close to or above rated wind speed (12 m/s). However, the damage contribution to the turbine is greater for higher wind speeds so that adapting the controller under these conditions shows the desired effects.

5.1 Setup of simulations

Simulations are performed using measured 10 minute wind data from the SCADA-system of a turbine in a near shore wind farm. The data is available for a period of 2 years and 10 months starting in summer. It is used for simulations using the described WT model (8) with a time step of $\Delta t_{sim} = 10\ min$. The trajectory of the desired health index over time HI_{des} is a major design parameter which needs to be determined within feasible limits of the selected controller configurations. In reality, it needs to be carefully selected by the turbine operator taking external influences like design parameters, maintenance planning and prices of electricity into account. The trajectory could also be changed during operation of the turbine. To evaluate the performance of the reliability controller, such external factors are neglected because it should be able to follow any predefined, feasible trajectory. To estimate the spent fatigue life budget and to create a feasible desired trajectory $HI_{des}(t)$, simulations of each of the 10 selected wind turbine controller configurations are performed. When linear degradation is assumed, the health index is expected to be 86 % after a simulation period of almost 3 years. However, most of the selected configurations still attain values higher than 95 %. One reason is that most of the selected configurations lead to reduced loads when compared to the default controller (see 3.4). Another reason can be deduced from statistical analysis of the wind data. Measured mean wind speeds and turbulence intensities at the turbine site are lower than the assumed wind conditions of an IEC class 3C site. This leads to lower degradation for all configurations. Therefore, design life times considerably longer than 20 years need to be selected in order to provide feasible HI-trajectories. On the one hand, this might not reflect reality entirely due to inaccuracy in the measured wind data and in the degradation model. On the other hand, it still indicates that degradation of the selected failure mode can be strongly reduced by derating strategies. Seasonal variations of the wind also strongly affect the degradation rate. Taking this into account, we select a piecewise linear desired health index where the slope is lower during summer (April to Oktober) than it is during winter. This approach is considered to be sufficient for the demonstration of the controller behavior.

Other design parameters refer to the MPC design itself. The cost function weights can exclusively be chosen to achieve the desired controller performance. Other parameters like the number of prediction steps p, the update rate of the controller t_s and the wind speed prediction t_w depend on external factors. These include quality and availability of wind predictions or available computing resources. For reasons of simplicity, the wind prediction is calculated as mean value of the simulated wind speeds and turbulence intensities with a time step of $t_w = k_w \Delta t_{sim}, k_w \in \mathbb{N}$. Applying this approach, the robustness of the controller to prediction errors is tested implicitly as the mean values cannot reproduce the fluctuations in the wind on a ten minute basis. The controller time step is selected to be a multiple $k_c \in \mathbb{N}$ of the wind prediction time step to prevent from additional interpolation. When t_s is given, the prediction horizon is determined by selecting the number of predictions steps p. This also defines the number of optimization variables, i.e. complexity of the optimization problem within the MPC. The global optimizer SHGO from the Python SciPy library is used as solver. A reasonable choice for the prediction horizon can be made by taking wind dynamics into account. According to van der Hoven (1957), there is a synoptic peak in the power spectrum of the wind between 4 and 10 days. Prediction horizons within that range are selected. Controller weights are selected so that sufficient reference tracking is assured while at the same time preventing the controller from unnecessary switching e.g. when the controller influence is low or not given due to low wind speeds.

5.2 Simulation results

In general, simulation results for a variety of parameters show that the desired health index can be controlled with the presented reliability control approach. A daily update of the real-time controller is sufficient to attain good results. Fig. 5 shows results for three different desired health index targets $HI_{des,32}$, $HI_{des,56}$ and $HI_{des,87}$ with a desired life times of 32, 56 and 87 years respectively (dashed lines). The corresponding current health indices from the simulation are denoted as $HI_{cur,32}$, $HI_{cur,56}$ and $HI_{cur,87}$. As a reference, uncontrolled simulations of the configuration with lowest DEL (config 1), with the nominal

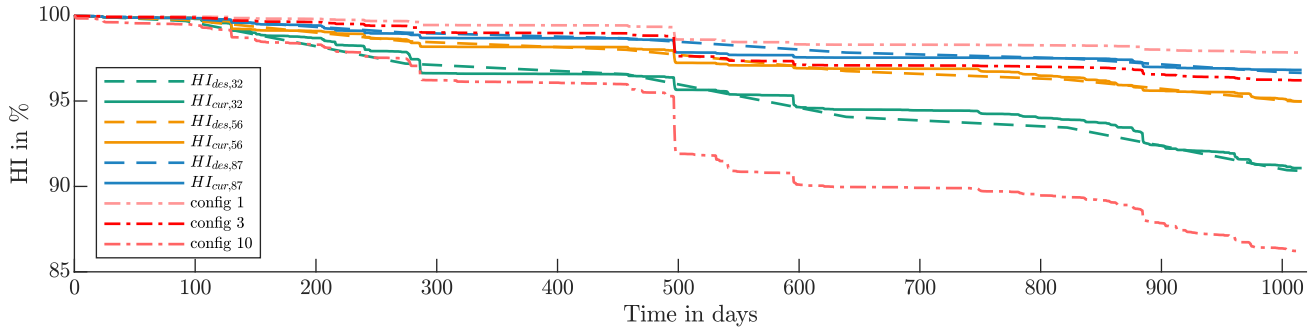

Fig. 5. Reliability controlled simulations for different targets of the desired health index

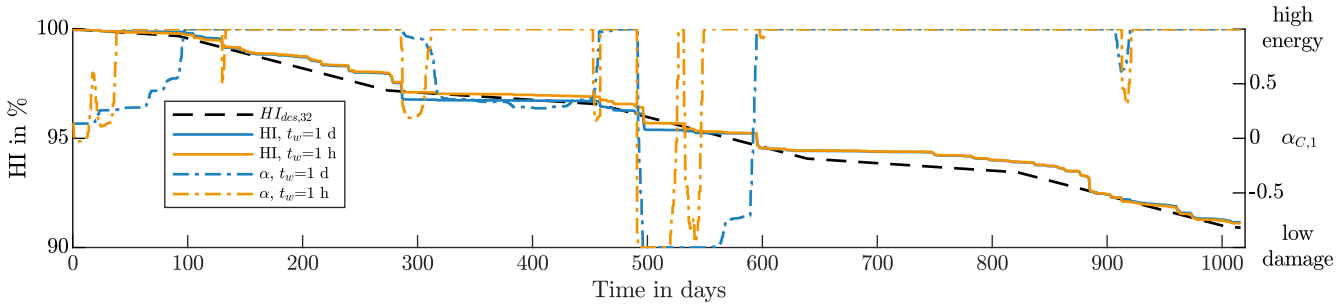

Fig. 6. HI (solid, left axis) and $\alpha_{C,1}$ (dash-dotted, right axis) for different wind prediction time steps

value for power $P_r = 7.5\ MW$ (config 3) and with the highest damage (config 10) are shown. The same value of $t_s = t_w = 1d$ is used for the time steps of the controller update and the wind prediction. The prediction horizon is 6 days, i.e. $p = 6$. The controller is clearly able to follow the desired setpoint. The energy yield is not shown in the figure, but increases as expected, when the HI decreases faster. When $HI_{des,32}$ is used, the energy yield over the simulated time span is e.g. about 5 % higher than for $HI_{des,56}$. However, fast changes in the HI can be observed e.g. in the middle of the simulation time after 500 days or after 284 days. This is caused by the wind and can not be prevented completely. The effect can be weakened by switching to the most preserving controller configuration 1. Still, such events or long periods of low wind speeds can cause a temporary deviation of the current health index from the desired health index. Nonetheless, it is possible to reduce this error consistently.

To examine the influence of the wind prediction, simulations for $HI_{des,32}$ are compared. The daily prediction ($t_w = 1d$, blue curves) is compared to an hourly prediction ($t_w = 1h$, orange curves). No other parameters are not changed. In particular, the prediction horizon and the step size remain the same. Fig. 6 shows the HI and the manipulative variable $\alpha_{C,1}$ of the corresponding simulations. Even though the course of the HI-trajectories is quite similar in general, a main difference can be seen at some particular points. Especially at day 284 of the simulation, the controller which uses hourly wind predictions reacts earlier. Therefore, the HI does not drop as much. This effect is examined in more detail in Fig. 7 where the simulated wind and HI-trajectory is compared to the predicted values from the MPC-controller. On the first half of day 286, the wind speed (ws) increases above 20 m/s. When the mean value is computed for a complete day, the prediction of wind speed and also the turbulence (TI) is much lower. Those values are then used for the prediction of HI which is shown as solid blue curve in the third plot of Fig. 7. Therefore, the HI is predicted to stay above the desired HI when the controller configuration with highest damage of $\alpha_C = 1$ is used. However, the simulated HI (dashed blue line) falls below the desired HI. A different behaviour can be observed when mean values are computed at each hour. In this case, a slight change in the manipulative variable, i.e. a change to a controller configuration with slightly lower damage, is sufficient to prevent the HI from falling below the desired value. Since the wind speed drops below 10 m/s from day 288 onwards, the influence of the controller is low and the damage rate of the turbine is reduced thereby. For this reason, α_C is not immediately reduced to a lower value close to -1. However, simulation results in Fig. 6 show that the early reaction allows the controller to switch to a configuration with higher energy earlier (orange dashed curve shortly after 300 days). When $t_w = 1d$ is used, the value of α_C (blue dashed curve) remains below 1 for almost 200 days.

In general, these results show that more accurate wind predictions increase the accuracy of the prediction and the controller performance. However, control errors due to inaccurate wind predictions can be corrected after sufficient times of ongoing simulation. Other simulations have shown that, by increasing the controller time step t_s, it is still possible to follow the desired health index, but at the cost of an increased control error. The control error can be slightly decreased by lowering t_s. To obtain the same prediction horizon T in this case, a larger number of prediction steps p, i.e. optimization variables for the optimal control problem, is necessary. This requires significantly more computing time. More efficient algorithms could be used to account for this. On a real wind turbine, however, solving the optimal control problem is not time critical because of the large time spans.

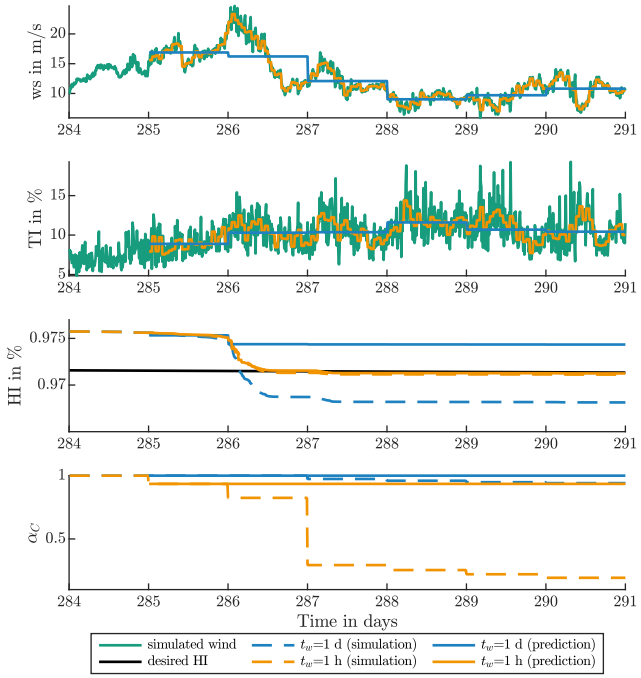

Fig. 7. Comparison of controller prediction (solid) and simulation (dashed) from day 284 onwards for different wind prediction time steps

6. CONCLUSION AND OUTLOOK

For the first time, the method of a supervisory reliability control was successfully applied to wind turbines. Simulation results show that the controller is able to control the desired degradation of the rotor blade fatigue loads independently of the provided desired set points.

In this paper, the complete process for the design and implementation of the reliability controller was presented. This includes the setup and solution of a multiobjective optimization problem to find suitable controller configurations. Using the results, the actual controller was designed. A prediction model and a verification model for the degradation of the selected failure mode of flapwise bending moments was created. In general, this research provides a proof for the applicability of reliability control to wind turbines and it offers extensive research potential in different areas. The robustness of the controller to prediction errors could be tested and improved. Other prediction models could also be implemented. To increase the potential of reliability control, more controller parameters of the real-time controller could be considered. Derating strategies in partial load of the turbines as well as parameters of fatigue reduction control strategies like IPC are candidates for this. However, more efficient strategies to solve the multiobjective optimization problem will then be required. In addition, control for more than one failure mode of the turbine will be required. Degradation or limits of other components like the tower, the drivetrain, the generator etc. need to be considered. On one hand, such information needs to be provided by a real wind turbine for realistic results. On the other hand, the reliability controller needs to be adapted so that more than one health index can be controlled. In order to do so, an $(m-1)$-dimensional parametrization can be used.

In the end, maximum profit is the ultimate objective for wind farm operators. Therefore, another field of future work is the transfer these results from one turbine to several turbines in a wind farm. In this case, the goal could be to have all turbines degrade with the desired health index and to maximize the energy production of the complete park at the same time. Additionally, more quantities such as maintenance planning and the costs involved as well as the price of electricity can be considered within the reliability controller itself or for the generation of setpoints.

REFERENCES

Beganovic, N., Njiri, J.G., and Söffker, D. (2018). Reduction of Structural Loads in Wind Turbines Based on an Adapted Control Strategy Concerning Online Fatigue Damage Evaluation Models. *Energies*, 11(12), 3429.

Bossanyi, E. (2018). Combining induction control and wake steering for wind farm energy and fatigue loads optimisation. *Journal of Physics: Conference Series*, 1037, 032011.

Galinos, C., Dimitrov, N.K., Larsen, T.J., Natarajan, A., and Hansen, K.S. (2016). Mapping Wind Farm Loads and Power Production - A Case Study on Horns Rev 1. In *Journal of Physics: Conference Series (Online)*, volume 753. doi:10.1088/1742-6596/753/3/032010. 032010.

IEC (2019). IEC 61400-1: Wind Turbines - Part 1: Design Requirements.

Krüger, M., Remirez, A., Kessler, J.H., and Trächtler, A. (2013). Discrete Objective-based Control for Self-Optimizing Systems. In *American Control Conference (ACC), 2013*, 3403–3408.

Leimeister, M. and Thomas, P. (2017). The OneWind Modelica Library for Floating Offshore Wind Turbine Simulations with Flexible Structures. In *Proceedings of the 12th International Modelica Conference*, 633–642. Linköping Electronic Conference Proceedings.

Meyer, T. (2016). *Optimization-based reliability control of mechatronic systems*. Ph.D. thesis, Universität Paderborn, Paderborn.

Meyer, T., Fischer, K., Wenske, J., and Reuter, A. (2017). Closed-loop supervisory control for defined component reliability levels and optimized power generation. In *Windeurope Conference and Exhibition 2017*. Windeurope, Amsterdam.

Njiri, J.G. and Söffker, D. (2016). State-of-the-art in wind turbine control: Trends and challenges. *Renewable and Sustainable Energy Reviews*, 60, 377–393.

Popko, W., Thomas, P., Sevinc, A., Rosemeier, M., Bätge, M., Braun, R., Meng, F., Horte, D., and Balzani, C. (2018). IWES Wind Turbine IWT-7.5-164. Rev 4. Bremerhaven.

Shokrieh, M.M. and Rafiee, R. (2019). 19 - Fatigue life prediction of wind turbine rotor blades. In A.P. Vassilopoulos (ed.), *Fatigue life prediction of composites and composite structures*, 681–710. WOODHEAD.

Sutherland, H.J. (1999). On the Fatigue Analysis of Wind Turbines. Albuquerque, New Mexico.

van der Hoven, I. (1957). Power Spectrum of Horizontal Wind Speed in the Frequency Range from 0.0007 to 900 Cycles per Hour. *Journal of Meteorology*, 14(2), 160–164.